Chaotic properties of the soft-disk Lorentz gas

J.C. Kimball
Physics Department, University at Albany, Albany, New York 12222
(Received 22 December 2000; published 24 May 2001)

The traditional hard-disk Lorentz gas describes the chaotic motion of a classical point particle through an array of impenetrable disks. Soft-disk modifications of the two-dimensional Lorentz gas, where the scattering particle can move into the disk interiors, are considered here. Conditions on the soft-disk potentials and disk separations that guarantee chaotic motion are obtained.

DOI: 10.1103/PhysRevE.63.066216 PACS number(s): 05.45.Ac, 05.20.Dd, 73.23.Ad

I. INTRODUCTION

Lorentz [1] proposed a simple model (now often called the Lorentz gas) to investigate the Drude theory of electrical conductivity in metals. Atoms in the metal were represented as fixed hard spheres which specularly scattered the electrons. Intuitively, one expects elastic scattering from the spherical atoms to quickly randomize the electron velocities. Proofs that the electron motion really is randomized by a lattice of scattering spheres are not easy. However, a number of exact result have been obtained for arrays of scattering disks in two dimensions [2–5], and more recent mathematical developments have been reviewed by Simanyi [6]. Results of these investigations reinforce our intuitive view of the approach to equilibrium. The Lorentz gas is ''chaotic,'' ''ergodic,'' and ''mixing,'' which means the motion is sensitive to initial conditions, time average approach spatial averages, and correlations decay in time (sometimes in an anomalous manner [7,8]).

Because atoms are not really hard spheres, one would like to know if more realistic scattering models are also chaotic, ergodic, or mixing. The chaotic aspect of this question is addressed here for ''soft-disk'' modifications of the two-dimensional Lorentz gas. We know from earlier numerical work that motion in the plane is not always chaotic or ergodic. Simulations have shown that planar motion of a particle in simple potentials is sometimes confined to special regions of phase space, as characterized by the KAM theorem [9]. Various aspects of potential scattering (with applications) are reviewed by Ott [10]. A discussion of soft-disk scattering with recent references is given by Donnay [11].

We will derive here two cases where soft-disk scattering does lead to chaos in the sense that adjacent paths diverge exponentially with the number of scattering events (an admittedly weak characterization of ''chaos''). Case 1 chaos occurs whenever each disk deflects the scattering path toward the disk center, and the magnitude of the deflection increases as the impact parameter decreases. A variety of attracting potentials with singularities at the origin, such as a truncated attracting Coulomb potential, can satisfy the condition for case 1 chaos. Case 2 chaotic systems have a more complicated characterization. The scattering path must be deflected away from the disk center, and the deflection angle must increase fairly rapidly as the impact parameter decreases. In addition, the disks may not touch, and there is a minimum disk separation (depending on the potential) that must be maintained for the system to be case 2 chaotic. The hard-disk Lorentz gas is a special limit of case 2 chaos. In this limit the minimum separation vanishes, as one expects. The demonstration of both types of chaos follows from two relatively simple recursion relations which will be derived in the following section.

II. RECURSION RELATIONS

A ''scattering'' recursion relation gives the bending of the particle's trajectory (as it moves through a disk) in terms of its impact parameter and the potential energy of the disk. The ''geometric'' recursion relation gives the change of the particle's impact parameter (as it moves from disk to disk) in terms of the geometry of the trajectory and the disk separations. The array of disks encountered by the scattering particle (labeled by an index j) are centered at positions $\vec{R}_j$. Each disk is characterized by its potential energy function $U_j(r)$ which depends only on the distance r from the disk center. Each disk has a radius a_j with $U_j(r)=0$ for $r>a_j$. The motion of the scattering particle is determined by classical mechanics and the total potential energy,

$$V(\vec{r})=\sum_j U_j(|\vec{r}-\vec{R}_j|). \tag{1}$$

A path that enters disk j is characterized by its incident angle ϕ_j and a signed impact parameter b_j (b_j being positive for paths traversing the disk in a counterclockwise direction). The same impact parameter characterizes the trajectory on entering and leaving a disk. To simplify notation, disks along a path are labeled sequentially, even though some disks may be visited more than once. After passing through disk j, the particle moves along a straight ''connecting line'' of length s_j to disk $j+1$ in a direction ϕ_{j+1}. When the particle enters the next disk, it is characterized by a new impact parameter b_{j+1}.

Different aspects of one example path segment are shown in Figs. 1, 2, and 3. To simplify the notation in these figures, the disk radii a_j and a_{j+1} are labeled ''a'' and ''a'.'' The impact parameters b_j and b_{j+1} and the angles ϕ_j and ϕ_{j+1} are similarly labeled.

A. Scattering recursion relation

In Figure 1 the path enters the larger disk moving in a direction ϕ with an impact parameter b, passes through the

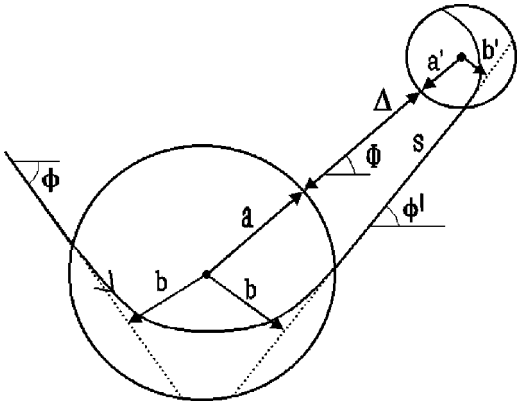

FIG. 1. A portion of a path (curve with large arrowhead) of a particle scattered by two attracting disks. The particle enters the first disk with an incident direction ϕ and leaves the disk in the direction ϕ'. The disk radii are a and a'. The impact parameters are b and b'. The disk separation line is labeled with its length Δ and its direction Φ. The connecting-line part of the path is labeled by its length s and its direction ϕ'.

disk (the curve with a large arrowhead), and leaves with the same impact parameter b but in a new direction ϕ'. Because the disk potential is isotropic, the difference between the incident and scattered directions can only depend on the potential $U(r)$ and the impact parameter b. That means $(\phi'-\phi)=\theta(b)$, where $\theta(b)$ is the ''scattering function'' for the larger disk. The generalization of this equation to an arbitrary disk gives the scattering recursion relation,

$$\phi_{j+1}=\phi_j+\theta_j(b_j), \tag{2}$$

where (for each disk j) the scattering function $\theta_j(b_j)$ is determined by the disk's potential $U_j(r)$. The characteristics of the scattering functions (plus the disk separations) determine whether or not the system can be chaotic, and the condition

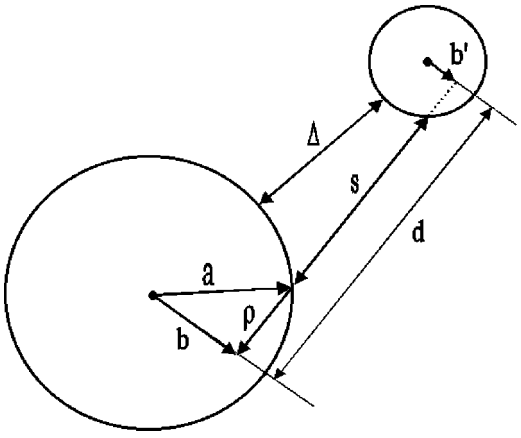

FIG. 2. Additional characterizations of the path of Fig. 1, with only the connecting-line portion of the path retained. The lines labeled with the lengths ρ, a,b in the larger disk form a right triangle. A ρ' is defined analogously for the smaller disk, but is not shown. The line with length $d=s+\rho+\rho'$ gives the length of the extended connecting line which terminates when it intersects the impact parameter lines labeled b and b'.

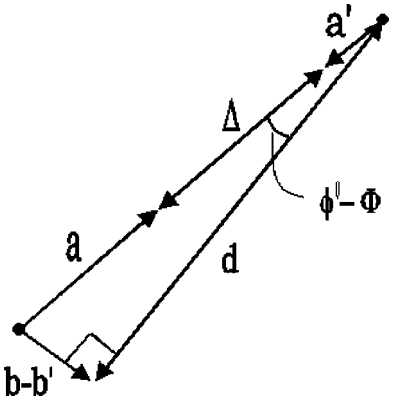

FIG. 3. A condensation of information from Figs. 1 and 2. The disk boundaries are not shown and the extended connecting line has been displaced so that one end is at the smaller disk's center. The angle between the two long legs of the resulting right triangle is $(\phi'-\Phi)$ and the short side of the triangle has length $(b-b')$.

for chaos will be expressed in terms of dimensionless functions $f_j(b_j)$ which are defined in terms of the derivative of the scattering function with respect to the impact parameter. With the index j suppressed,

$$f(b)=\rho\frac{\partial\theta}{\partial b}, \tag{3}$$

where $\rho=\sqrt{a^2-b^2}$ is half the distance the particle would travel inside the disk if it were undeflected. This distance is shown for the larger disk of Fig. 2. We consider potentials sufficiently well behaved so that $f(b)$ is defined (except at isolated points, such as $b=0$).

B. Geometric recursion relation

Referring again to Fig. 1 we note that after being scattered by the larger disk, the particle moves along the straight ''connecting line'' (labeled by its length s and direction ϕ'), enters the smaller disk with an impact parameter b', and then is scattered by the smaller disk. Also shown in Fig. 1 is the ''disk separation line,'' labeled by its length Δ and its direction Φ.

In Fig. 2 only the connecting-line portion of the scattering particle's path is shown. Also shown in the larger disk of Fig. 2 is a triangle with sides ρ and b and hypotenuse a, so $\rho=\sqrt{a^2-b^2}$. A corresponding $\rho'=\sqrt{(a')^2-(b')^2}$ is defined for the smaller disk, but ρ' is not shown to avoid clutter. The line labeled with length d in Fig. 2 denotes the length of an ''extended connecting line'' whose end points are the perpendicular intersections with the impact parameter lines b and b'. The length of the extended connecting line is $d=s+\rho+\rho'$.

In Fig. 3 the disk surfaces are not shown, but lines and angles from Figs. 1 and 2 are used to illustrate the geometric recursion relation of Eq. (4). The extended connecting line of length d in Fig. 3 has undergone a parallel displacement so that one end is at the center of the smaller disk. The length of the line between the disk centers is the sum of the disk radii $(a+a')$ plus the length of the disk separation line Δ. The

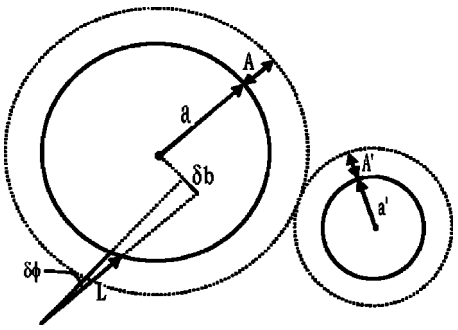

FIG. 4. Two infinitesimally differing paths, characterized by the angle difference $\delta\phi$ and the impact parameter difference δb approach the left-hand disk. For this example, the paths converge at a point a distance L from the disk's surface. Also shown are a second disk and the shell thicknesses A and A' which enforce a minimum separation $(A+A')$ between disks.

angle between the lines d and $(a+a'+\Delta)$ is $(\phi'-\Phi)$, as can be seen from Fig. 1. The third side of the right triangle in Fig. 3 has length $(b-b')$ and $(b-b')$ is perpendicular to d. Thus $(b-b')=(a+\Delta+a')\sin(\phi'-\Phi)$. This is the abbreviated version of the geometric recursion relation. With subscripts restored, it reads

$$b_{j+1}=b_j-(\Delta_j+a_j+a_{j+1})\sin(\phi_{j+1}-\Phi_j). \tag{4}$$

The recursion relations of Eqs. (2) and (4) will be used to derive the two classes of chaos described in the following section.

III. CHAOS

A chaotic (or hyperbolic) system is characterized by an exponential growth in the separation of nearly all adjacent paths. Consider two paths that enter disk j with infinitesimally differing directions $\delta\phi_j$ and infinitesimally differing impact parameters δb_j (see Fig. 4). These paths arrive at disk $j+1$ with a new angle difference $\delta\phi_{j+1}$ and a new impact parameter difference δb_{j+1}, given by

$$\begin{pmatrix}\delta\phi_{j+1}\\ \delta b_{j+1}\end{pmatrix}=M_j\begin{pmatrix}\delta\phi_j\\ \delta b_j\end{pmatrix}, \tag{5}$$

where M_j is the matrix obtained by linearizing the recursion relations of Eqs. (2) and (4). Abbreviating $f_j(b_j)$ from Eq. (3) by f_j,

$$M_j=\frac{\partial(\phi_{j+1},b_{j+1})}{\partial(\phi_j,b_j)}=\begin{pmatrix}1 & f_j/\rho_j\\ -d_j & 1-d_jf_j/\rho_j\end{pmatrix}, \tag{6}$$

where the differentiation gives $d_j=(\Delta_j+a_j+a_{j+1})\cos(\phi_{j+1}-\Phi_j)$. One can see from the trigonometry of Fig. 3 that this is the same d_j that appears in Figs. 2 and 3, so

$$d_j=s_j+\rho_j+\rho_{j+1}. \tag{7}$$

If a path passes through N disks, the linearized map is the matrix product $M_N\cdots M_2M_1$.

The matrices of Eq. (6) determine whether or not the system will be chaotic, and the properties of the disk potentials appear only through the term f_j in these matrices. We consider two cases where chaos (meaning the exponential separation of adjacent paths caused by repeated scattering events) is assured for essentially all paths.

A. Case 1: Negative *f*

If the f_j are negative for all values of the impact parameters b_j, then the off-diagonal elements of each M_j are negative and the lower right element of each M_j is greater than unity. Taking $\delta\phi_1=0$ and $\delta b_1>0$ yields a lower bound on the impact parameter difference after N iterations of the recursion relations,

$$\delta b_{N+1}\geqslant\delta b_1\prod_{j=1}^{N}\left(1-\frac{d_jf_j}{\rho_j}\right). \tag{8}$$

One obtains this lower bound by ignoring the $\delta\phi_j$ produced after each matrix multiplication. Inclusion of the $\delta\phi_j$ can only increase δb_{N+1}.

The lower bound of Eq. (8) is path dependent. It depends on which disks scattered the particle as well as the impact parameters along the path. We can use this lower bound to establish a minimum separation between adjacent paths which depends only on the disks along the path, and not the impact parameters. This alternative lower bound makes it clear that negative f_j mean paths will continue diverging from each other as long as the collisions persist. Using $d_j>\rho_j+\Delta_j$ and $a_j\geqslant\rho_j$ [see Eq. (7) and Fig. 2] an alternative lower bound on the δb_j is

$$\delta b_{N+1}\geqslant\delta b_1\prod_{j=1}^{N}\left(1+Z_j\left[1+\frac{\Delta_j}{a_j}\right]\right), \tag{9}$$

where

$$Z=\min_b[-f(b)]. \tag{10}$$

B. Case 2: *f*>1 and a minimum separation

This case is more complicated because there are two criteria for chaos. First, one must have $f_j>1$ for all disks. Second, there is a lower bound on the disk separation (labeled Δ in Figs. 1 and 2). As will be show below, this minimum distance can be maintained if each disk is surrounded by an impenetrable ''shell'' of thickness A_j (see Fig. 4). The minimum separation (or shell thickness) depends on the disk potentials, and it vanishes for an array of hard disks.

It is convenient to introduce new distances x_j which relate the impact parameter differences to the angle differences through

$$\delta b_j=-\frac{2}{f_j}(x_j+\rho_j)\,\delta\phi_j. \tag{11}$$

Physically, a positive x_j describes paths diverging from a point which is a distance $L=(2x_j+\rho_j[2-f_j])/f_j$ from the

point of impact with sphere j, as is illustrated in Fig. 4. Expressing the linearized recursion relations in terms of the x_j gives two expressions equivalent to Eq. (5). The first is

$$\delta\phi_{j+1} = -\left(1+\frac{2x_j}{\rho_j}\right)\delta\phi_j . \tag{12}$$

Thus the condition for chaos ($|\delta\phi_{j+1}|>|\delta\phi_j|$) will be satisfied if all the $x_j>0$. The second expression is

$$\frac{2x_{j+1}}{f_{j+1}} = s_j - \rho_{j+1}\left(\frac{2}{f_{j+1}}-1\right) + \left[2x_j\left(1-\frac{1}{f_j}\right)-\rho_j\left(\frac{2}{f_j}-1\right)\right]\left(1+\frac{2x_j}{\rho_j}\right)^{-1}. \tag{13}$$

Starting with a positive x_0, the x_j will be positive for all $j>0$ provided the two conditions of case 2 chaos (described in the following two equations) are satisfied. The first condition is

$$f_j > 1. \tag{14}$$

The second is

$$s_j > \rho_j\left(\frac{2}{f_j}-1\right)+\rho_{j+1}\left(\frac{2}{f_{j+1}}-1\right). \tag{15}$$

Since $s_j \geqslant \Delta_j$ (see Fig. 1) this condition on s_j will be satisfied if each disk is surrounded with a shell of thickness A_j given by

$$A = \max_b\left(\rho(b)\left(\frac{2}{f(b)}-1\right)\right). \tag{16}$$

If disk shells are not allowed to overlap, as is shown in Fig. 4, the minimum space between the disks is

$$\Delta_j^* = A_j + A_{j+1}. \tag{17}$$

As with case 1, a lower bound on the growth of the scattering angle difference can be obtained which is independent of the impact parameters. Using the alternate form of the linearized recursion relations [Eqs. (12) and (13)], and the inequalities $f_j>1$, $a_j \geqslant \rho_j$, and $s_j \geqslant \Delta_j$ one obtains

$$|\delta\phi_{N+1}| > |\delta\phi_1| \prod_{j=1}^{N}\left(1+\left[\frac{\Delta_j-\Delta_j^*}{a_j}\right]\right). \tag{18}$$

IV. EXAMPLES

The scattering function $\theta(b)$ for a particle in a central potential $U(r)$ is obtained from basic mechanics. Using units where the particle's energy is $E=1$ and its mass is $\mu=1/2$, the particle has unit velocity and an angular momentum (with respect to a disk center) which is half the impact parameter. For this case (see [12])

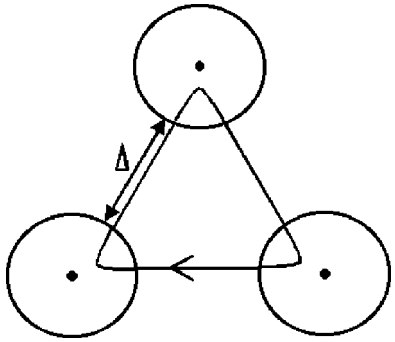

FIG. 5. An example periodic orbit which changes from stable to class 2 chaotic as the disk separation Δ is increased.

$$\theta(b) = -2\cos^{-1}(b/a) + 2\int_{r_c}^{a}\frac{b/r^2}{\sqrt{1-U(r)-[b/r]^2}}dr, \tag{19}$$

where r_c is the distance of closest approach. We consider power-law and truncated Coulomb potentials where simple expressions for the scattering angles can be obtained.

A. Power-law potential

The power-law potential is

$$U(r)_p = \begin{cases} 1-(r/a)^p, & r<a \\ 0, & r\geqslant a, \end{cases} \tag{20}$$

where one must have $p>-2$ to avoid paths which fall to the disk center. Physically, paths produced by this example also describe the classical propagation of a light beam through an array of dielectric disks with indices of refraction $n(r) = (r/a)^{p/2}$.

The scattering function can be evaluated for the power-law potential, giving

$$\theta(b) = \frac{-2p}{p+2}\cos^{-1}\left(\frac{b}{a}\right), \tag{21}$$

which means $f(b)$ is independent of the impact parameter

$$f = \frac{2p}{(p+2)}. \tag{22}$$

This means case 1 chaos occurs for the power-law potential when p is negative. The lower bound on the exponential separation between adjacent paths is given by Eq. (10) with $Z=2p/(p+2)$. Case 2 chaos occurs if $p>2$ and the minimum disk separation is enforced by a shell thickness

$$A = \frac{2a}{p}. \tag{23}$$

B. Periodic orbit

The periodic orbit shown in Fig. 5 illustrates case 2 chaos for the power-law potential. Three identical disks with identical power-law potentials are placed at the corners of an

equilateral triangle with side $2a+\Delta$. The periodic orbit sketched in Fig. 5 can only occur when $p>4$, so the $f>1$ condition for case 2 chaos is automatically satisfied. However, one must still consider the disk separation. Since the three disks, scattering angles, and distances are identical, the stability of this system is determined by the eigenvalues of a single matrix M [Eq. (6)]. The motion will be chaotic when the modulus of one of the eigenvalues of M is greater than unity. This happens when the magnitude of the trace of M is greater than 2. Using Eq. (21) with $\theta=-2\pi/3$ gives $\rho = a\cos[\pi(p-4)/(6p)]$, so

$$\mathrm{Tr}\{M\}=2-\left(\frac{2p}{p+2}\right)\frac{2a+\Delta}{a\cos[\pi(p-4)/(6p)]}. \tag{24}$$

The requirement that $\mathrm{Tr}\{M\}<-2$ for instability means both separation (larger Δ) and hardness (larger p) are needed to assure chaos. The criterion for instability of the path shown in Fig. 5 requires a smaller disk separation than is implied by the shell thickness specified in Eq. (23) because Eq. (23) is the more general condition for the instability of all paths.

A system with just one stable periodic orbit is not ergodic. Thus one cannot assume ergodic behavior of a randomly distributed array of soft disks that satisfy the $f>1$ condition of case 2 chaos because a few of the disks may sit close together and allow stable periodic orbits.

C. Coulomb potential

The truncated Coulomb potential is

$$U(r)_\gamma=\begin{cases}\gamma(a/r-1), & r<a\\ 0, & r\geqslant a\end{cases} \tag{25}$$

with the parameter γ giving the sign of the potential (attraction or repulsion) as well as the potential strength.

The integral that gives the scattering angle for this Coulomb potential is tabulated [13]. Differentiating the result with respect to the impact parameter gives

$$f(b)=\frac{\gamma(1+\gamma/2)}{(1+\gamma)(b/a)^2+(\gamma/2)^2}. \tag{26}$$

The negative f condition means the system will be case 1 chaotic when $-2<\gamma<0$. When γ is in this range a lower bound on the exponential growth rate, which is independent of angles and impact parameters, is given by Eq. (9) with

$$Z=\begin{cases}-\gamma/(1+\gamma/2), & -1<\gamma<0\\ -(1+\gamma/2)/\gamma, & -2<\gamma<-1.\end{cases}$$

For case 2 chaos, the $f>1$ condition is satisfied if $\gamma>2$ or $\gamma<-4$. A shell thickness

$$A=\begin{cases}\dfrac{a}{\gamma}\dfrac{2\sqrt{2}}{3\sqrt{3}}\sqrt{\dfrac{2+\gamma}{1+\gamma}}, & \gamma>2\\ \dfrac{-2a}{2+\gamma}, & \gamma<-4\end{cases}$$

is sufficient to assure case 2 chaos.

D. Hard disks

The hard-disk Lorentz gas is a limit of case 2 chaos with $f=2$. This value for f can be obtained from a geometric construction. It can also be obtained from the $p\to\infty$ limit of the power-law potential or the $|\gamma|\to\infty$ limit of the truncated Coulomb potential. For hard disks, the recursion relations for $\delta\phi_j$ and x_j [Eqs. (12) and (13)] simplify to

$$\delta\phi_{j+1}=-\left[1+\frac{2x_j}{\rho_j}\right]\delta\phi_j \tag{27}$$

and

$$x_{j+1}=s_j+\left(\frac{x_j}{2x_j+\rho_j}\right)\rho_j. \tag{28}$$

In this hard disk limit, one is assured that an initial positive x_0 will lead to positive x_j for all $j>0$, with no lower bound on the space between disks. An alternative and readable derivation of expressions equivalent to Eq. (28) (obtained by Sinai) is given by Gaspard [14]. A formal solution to Eq. (28) can be written as a continued fraction.

E. Low density disk arrays

If the separations between disks Δ_j are always large (but never infinite) compared to the disk radii a_j, then it is convenient to express the divergence of paths in terms of an approximate Lyapunov exponent λ. For case 1, after a time t,

$$\delta b(t)\approx\delta b(0)\exp(\lambda t), \tag{29}$$

where

$$\lambda\gtrsim\lim_{N\to\infty}\frac{\sum_{j=1}^{N}\ln(1+Z_j\Delta_j/a_j)}{\sum_{j=1}^{N}\Delta_j}. \tag{30}$$

For case 2, the same approximate lower bound for λ is obtained, except $Z_j\to 1$. For either case, a soft-disk version of the Krylov conjecture [15] for the Lyapunov exponent can be extracted from this approximate bound on λ. After replacing a_j with an average a, Z_j with an average Z, and Δ_j with a ''typical'' mean free path $\alpha/(na)$, where n is the density of scattering sites and α is a number on the order of unity, one obtains a simplification of Eq. (30) consistent with the observation that λ should be of order $|n\ln(n)|$ for small n,

$$\lambda \gtrsim \frac{na}{\alpha} \ln\left(1 + \frac{Z\alpha}{na^2}\right). \tag{31}$$

We emphasize again, however, that a randomly distributed array of disks for case 2 may not be chaotic or ergodic because a few stable periodic orbits may occur for disks that happen to sit in close proximity.

V. COMMENTS

The case 1 examples of chaos were realized using attracting potentials with singularities at the origin. This is not a coincidence because a negative f is generally associated with an attracting potential. A $U(\vec{r})$ which is continuous, attracting, and bounded will have a vanishing scattering angle for $b \to 0$ and for $b \to a$. Thus the scattering angle could not decrease over the whole range of impact parameters. However, a large class of potentials which are singular at the origin, so the scattering angle is not a continuous function of the impact parameter as $b \to 0$, can be found which satisfy the $f < 0$ criterion.

The Coulomb potential with large negative γ approaches the hard-disk result because the highly eccentric elliptic orbit produced by this strongly attracting potential returns the scattering particle to nearly the same position on the disk surface. Furthermore, the particle leaves the disk moving in a direction nearly equivalent to the direction obtained for hard-disk scattering. Generally speaking, other attracting potentials do not have this property.

We have done extensive numerical tests on periodic disk arrays that are described by the recursion relations of Eqs. (2) and (4). In every case tested, systems that are either case 1 or case 2 chaotic also appear to be ergodic. Of course this is not a proof of ergodicity.

We speculate that qualitative results obtained here apply more generally to real systems where the potentials do not vanish in the inter-disk region. For example, the observation that weakly attracting truncated Coulomb potentials are class 1 chaotic, while only relatively strong repelling Coulomb potentials can be Class 2 chaotic, may be another reason why the crystal channeling of energetic particles is much less effective when the channeled particles are negative.

ACKNOWLEDGMENTS

I am happy to acknowledge Professor Harry Frisch for his encouragement and suggestions which changed the emphasis of this work. I also wish to thank Dr. Marco Lenci and Dr. V.J. Donnay for useful suggestions.

[1] H.A. Lorentz, Arch. Neerl. **10**, 336 (1905) [reprinted in *Collected Papers* (Nejhoff, The Hague, 1936), Vol. III, p. 180].
[2] J.L. Lebowitz, in *Transport Phenomena*, edited by J. Ehlers, K. Hepp, and H.A Weidenmuller (Springer-Verlag, New York, 1974).
[3] L.A. Bunimovich and Ya.G. Sinai, Commun. Math. Phys. **78**, 479 (1981).
[4] L.A. Bunimovich, Ya.G. Sinai, and N.I. Chernov, Russ. Math Surv. **46**, 46 (1991).
[5] N.I. Chernov and C. Haskell, Ergod. Theory Dyn. Sys. **16**, 19 (1996).
[6] N. Simanyi, Ergod. Theory Dyn. Sys. **19**, 741 (1999).
[7] T.E. Wainright, B.J. Alder, and D.M. Gass, Phys. Rev. A **4**, 233 (1971).
[8] P.L. Krapivsky and S. Redner, Phys. Rev. E **56**, 3822 (1997).
[9] T. Geisel, A. Zacherl, and G. Radons, Phys. Rev. Lett. **59**, 2503 (1987); Z. Phys. B: Condens. Matter **71**, 117 (1988).
[10] E. Ott, *Chaos in Dynamical Systems* (Cambrige University Press, Cambridge, England, 1993), Secs. 5.4 and 5.5.
[11] V.J. Donnay, J. Stat. Phys. **96**, 1021 (1999).
[12] J.B. Marion and S.T. Thornton, *Classical Dynamics of Particles and Systems*, 4th ed. (Saunders, Fort Worth, 1995), p. 369.
[13] I.S. Gradshteyn and I.M. Ryzhik, *Table of Integrals, Series, and Products*, 5th ed. (Academic Press, Boston, 1994), No. 2.266.
[14] P. Gaspard, *Chaos, Scattering and Statistical Mechanics* (Cambridge University Press, Cambridge, England, 1998), Chap. 1.
[15] N.S. Krylov, *Works on the Foundations of Statistical Physics* (Princeton University Press, Princeton, NJ, 1979).